Biospheric feedback effects in a synchronously coupled model of Earth and human systems

Authors: Peter E. Thornton[*], Katherine Calvin, Andrew D. Jones, Alan V. Di Vittorio, Ben Bond-Lamberty, Louise Chini, Xiaoying Shi, Jiafu Mao, William D. Collins, Jae Edmonds, Allison Thomson, John Truesdale, Anthony Craig, Marcia L. Branstetter, George Hurtt [†]

Fossil fuel combustion and land-use change are the two largest contributors to industrial-era increases in atmospheric CO_2 concentration[1]. Projections of these are thus fundamental inputs for coupled Earth system models (ESMs) used to estimate the physical and biological consequences of future climate system forcing[2,3]. While historical datasets are available to inform past and current climate analyses[4,5], assessments of future climate change have relied on projections of energy and land use from energy economic models, constrained by assumptions about future policy, land-use patterns, and socio-economic development trajectories[6]. Here we show that the climatic impacts on land ecosystems drives significant feedbacks in energy, agriculture, land-use, and carbon cycle projections for the 21st century. We find that exposure of human appropriated land ecosystem productivity to biospheric change results in reductions of land area used for crops; increases in managed forest area and carbon stocks; decreases in global crop prices; and reduction in fossil fuel emissions for a low-mid range forcing scenario[7]. The feedbacks between climate-induced biospheric change and human system forcings to the climate system – demonstrated here – are handled inconsistently, or excluded altogether, in the one-way asynchronous coupling of energy economic models to ESMs used to date[1, 8-9].

[†] Present addresses: P.E.T., X.S., and J.M., Oak Ridge National Laboratory, Environmental Sciences Division/Climate Change Science Institute; K.C., B.B.-L., and J.E., Joint Global Change Research Institute, Pacific Northwest National Laboratory; A.D.J., A.V.D., and W.D.C., Lawrence Berkeley National Laboratory; L.C. and G.H., University of Maryland; J.T. and A.C., independent contractors with Lawrence Berkeley National Laboratory; M.L.B., Oak Ridge National Laboratory, Computer Science and Mathematics Division/Climate Change Science Institute; A.T., Field to Market: The Alliance for Sustainable Agriculture, 777 N Capitol St NE, Washington, DC 20002. [*] Corresponding author, contact information: thorntonpe@ornl.gov.

Current projections of future climate are based on ESMs that include sophisticated representations of biotic and abiotic processes in the Earth system, but which represent human systems through static, unidirectional, asynchronous coupling[10] (black arrows in Figure 1a). We explore here the difference between asynchronous coupling, in which human system models are executed in advance to generate complete time series outputs later passed to an ESM, and synchronous coupling, in which the human system model and ESM are executed simultaneously, with opportunity for interaction between these two components that can change the simulation trajectory of both. In the traditional asynchronous approach, human system information required as forcing for climate prediction is generated in advance by economic integrated assessment models (IAMs) that include both energy and agricultural sectors. As summarized in the Fifth Assessment Report of the Intergovernmental Panel on Climate Change (AR5), several IAMs have been used to generate standard climate forcing inputs to ESMs covering a range of policy assumptions from aggressive mitigation to business-as-usual[1,11]. These inputs include harmonized forcings sharing a common historical baseline and a common set of definitions and analyses for 21st century long-lived[12] and short-lived[13] greenhouse gas (GHG) emissions and land-use change[5].

IAM projections of future GHG and air pollutant emissions and land-use and land-cover change (LULCC) are constrained by assumptions regarding human demography, economic development trajectories, and policy. Estimates of ecosystem productivity and crop yields (including biomass energy crops for some scenarios) are based on historical data. These estimates change over time, following assumptions about the influence of technological change on yield and endogenous estimates of crop location and area (Figure 1a). IAMs do not typically consider the influence of future biospheric change, defined here as the integrated effects of climatic, ecological, and biogeochemical processes, although recent work has evaluated the economic and carbon stock impacts of changing temperature, precipitation, and atmospheric carbon dioxide concentration ($CO_{2,atm}$) in crop and land-use models[14,15].

The use of asynchronous coupling in climate projections for AR5 excludes the influence of multiple biospheric factors known to influence managed ecosystems, including short-term weather variation[16], long-term climate trends[17], changes in $CO_{2,atm}$[18,19], changes in atmospheric deposition of reactive nitrogen on land[20], and the complex interactions among these factors[21,22]. One IAM used in AR5, the IMAGE model, does have the capability to examine the dynamic influence of climate change factors on ecosystem productivity using its own internal, reduced-form climate model[23], but its scenarios for use by ESMs are still based on one-way coupling and result in inconsistent representation of biospheric change between the IAM and ESM. Two-way coupling of IMAGE to a general circulation model (GCM) was used to examine changes in land use[24], but the feedback in that case was limited by passing only 30-year mean monthly temperature and precipitation changes from the GCM to IMAGE. In that study, simulation of carbon cycle and ecosystem processes was performed within IMAGE, a simple and highly parameterized land model which ignores the tight integration of biophysical and biogeochemical processes, driven by sub-daily variations in temperature, precipitation, humidity, and short and long-wave radiation. Mechanistic coupling of biological and physical processes at the land surface-atmosphere interface is a defining feature of the current generation of ESMs[1].

Here we investigate the influence of biospheric change on human systems and associated feedbacks to the biosphere as introduced in a synchronous two-way coupling approach. We accomplish two-way coupling by passing biospheric change information from an ESM to the ecosystem productivity and crop yield components of an IAM at five-year intervals, as radiatively-forced climate change unfolds over the course of a 90-year simulation (2005-2094). We examine the consequences of realistic two-way feedback between the human and Earth system components for crop price, fossil fuel emissions, LULCC, and transfers of carbon between land, ocean, and atmosphere (Figure 1b). The IAM component used here is the Global Change Assessment Model (GCAM 3.0)[25] and the ESM is the Community Earth System Model (CESM 1.1)[26]. We refer to the two-way coupled system as the integrated Earth system model (iESM)[27]. Our investigation uses the same demographic and policy assumptions as the 4.5 W m^{-2} radiative forcing reference concentration pathway (RCP4.5) scenario of AR5[7], which was originally generated by GCAM. The passing of LULCC signals from IAM to ESM is based on the land-use harmonization approach used in AR5[5], with modifications to improve signal integrity[8]. To help assess the generality of our results, we also performed a pair of simulation experiments based on the AR5 RCP 8.5 scenario.

[insert Figure 1 here]

Coupling from ESM to IAM is accomplished by passing an integrated biospheric change signal to each of the IAM spatial units and land types at five-year intervals. This signal is based on departures from a present-day baseline (average over period 2000-2004) of net primary production and heterotrophic respiration generated by the ESM land model component, which includes a fully prognostic treatment of energy, water, carbon, and nitrogen cycles for multiple vegetation types in each ESM land grid cell. This signal captures the desired change factors with minimal bias and a linear response, while minimizing signal interference from LULCC[28].

The global average of the productivity and yield component of this signal is similar in magnitude and time course among the major vegetated land types, increasing by about 10% by 2094 (Figure

2), with regional variation reflecting patterns of changed ecosystem productivity in the ESM (Supplemental Figure 2). In CESM, land productivity tends to increase under climate change scenarios, driven primarily by increasing atmospheric CO_2 concentration and anthropogenic nitrogen deposition associated with fossil fuel combustion, overlain with spatially and temporally varying effects due to increasing temperature and changing precipitation patterns. Even though CESM, with its inclusion of carbon-nitrogen cycle coupling, generates one of the lowest CO_2 fertilization effects in the CMIP5 collection of ESMs, the CO_2 fertilization effect still dominates the varying climate feedbacks to produce global-scale patterns of increasing land productivity under all tested scenarios[1]. Nothing we have added to the iESM system alters these ESM-centric aspects of the ecosystem-climate feedbacks, and the increasing productivity obtained in our iESM experiments is qualitatively and quantitatively consistent with the well-characterized behavior of CESM in this regard. The unique aspect of our study is that this increased productivity is communicated synchronously to the human system component to influence LULCC (and other energy economic factors such as crop price and fossil fuel emissions). Our estimate of 10% increase in ecosystem productivity and crop yield over present-day is consistent with estimates from free-air CO_2 enrichment (FACE) studies for crop yield[18]. $CO_{2,atm}$ prognosed in the ESM rises to approximately 590 parts per million by volume by 2094 in the two-way coupled simulation (Supplemental Figure 3), similar to the enriched levels typical of FACE experiments, although a direct comparison of model and experimental results in this case suffers from differences in the time scale of changed forcing and the integration in our simulations of additional factors such as changing climate and changing rates of nutrient inputs and mineralization. Our finding of increased productivity under future climate change contrasts with recent results reported for a comparison of agricultural models, but that study excluded the possibility of CO_2 fertilization[14]. Other recent work has stressed the importance of modeled nutrient dynamics in estimating CO_2 fertilization for global cropland[22], a factor included in our ESM.

[insert Figure 2 here]

We quantify the influence of coupling approaches by differencing two simulations, one with two-way synchronous coupling and the other with traditional one-way asynchronous coupling. A common trajectory for fossil fuel emissions is used in both simulations (discussed below). Global crop prices increase through 2080 for both coupling approaches under RCP4.5, driven by a mitigation policy that applies a cost to carbon emissions[25] (Supplemental Figure 4), but the increase in price is 12-25% smaller in the synchronously coupled system (Figure 3a), with similar magnitude and trajectory for major crop types. The decline in prices under the experimental simulation is due to higher productivity (Supplemental Figure 5) that reduces cropland requirements and lessens competition for land. Higher productivity with biospheric feedback drives a 10% decrease in total global crop area, as the same amount of food and feed can be produced on smaller amounts of land. The decrease in total global crop area is accompanied by an increase in area of noncommercial forest (Figure 3b).

[insert Figure 3 here]

These changes drive carbon cycle responses in the land model component of the ESM, resulting in altered $CO_{2,atm.}$ Atmospheric change drives additional response in the ocean carbon cycle through physical and biological feedbacks with $CO_{2,atm}$ (Figure 1b, pathways labeled 3, 4, and 5). Specifically, land ecosystems accumulate 5-10 Pg of additional carbon with two-way coupling, driving a decrease in $CO_{2,atm}$ that in turn reduces the amount of carbon transferred from the atmosphere to the ocean by ~3 Pg C (Figure 4). Variability in this feedback flux on interannual to decadal timescales is suggested by the two ensemble members, superimposed on a coupling signal with peak increase in land carbon storage around 2060. This peak and subsequent decline corresponds in time with a reduced rate of increase in non-commercial forest area (Figure 3b). An important caveat for our study is that the ESM component of our coupled system does not include a detailed crop model, and treats crops as grassland types.

[insert Figure 4 here]

Increases in ecosystem productivity and crop yield, combined with decreases in the global land area required for food, feed, and fiber crops drive increases in bioenergy potential and corresponding decreases in the price of bioenergy. The decline in bioenergy cost results in an increase in demand, an increase in land area dedicated to biomass energy production (Figure 3b), and a decline in the demand of other energy carriers (e.g., gas and coal). The decrease in carbon-intensive energy production leads to a 17% reduction in projected fossil fuel emissions by the end of the 21st century (Supplemental Figure 6). The changes in global carbon stocks shown in Figure 4 do not reflect the lower fossil fuel emissions generated by the biospheric feedback, as we held these emissions constant for the two simulations to provide the least complicated feedback demonstration. We expect that a more complete coupling, in which the updated fossil fuel emissions are passed to the ESM, would result in lower atmospheric concentrations, less land carbon storage via CO_2 fertilization in the ESM land model, and a decreased rate of ocean carbon uptake.

We obtain qualitatively similar results when comparing asynchronous one-way coupling and synchronous two-way coupling under a higher radiative forcing scenario (RCP 8.5). Biospheric change caused increases in crop yield of 15-22% for RCP 8.5, compared to 11-17% increase for RCP 4.5 (Supplemental Figure 7). Two-way coupling causes a decrease in crop prices of 6-17% for RCP 8.5, compared to 12-25% decrease for RCP 4.5. Changes in yield and price drive shifts in LULCC that are somewhat larger for RCP 8.5 than for RCP 4.5, while acting through similar mechanisms. The land ecosystem accumulates an additional 5-10 PgC due to two-way coupling by the final decades of RCP 8.5, comparable to the additional accumulation for RCP 4.5.

We conclude that biospheric feedbacks to human systems can significantly alter primary anthropogenic climate forcing by driving changes in land use and energy activities which propagate to changes in land, atmosphere, and ocean carbon stocks as well as changes in fossil fuel emissions trajectories: truly comprehensive climate change assessment efforts must therefore consider these feedbacks. The approach demonstrated here removes a major inconsistency in the practice of coupled Earth system modeling as identified in AR5[1], thereby improving the policy relevance of climate and Earth system model projections[29,30]. Our study does not seek to provide a comprehensive assessment of uncertainty associated with a particular scenario. Indeed, a synchronously coupled system that includes an ESM component can never replace the traditional use of stand-alone IAMs as tools for deep exploration of uncertainty. Instead, we argue that the synchronously coupled system is a new tool that allows us to explore a previously dark region of the uncertainty space: each time an ESM is run without synchronous coupling we miss an opportunity to better understand and quantify this uncertainty.

References

1 IPCC. *Climate Change 2013: The Physical Science Basis. Contribution of Working Group I to the Fifth Assessment Report of the Intergovernmental Panel on Climate Change* (eds T.F. Stocker *et al.*) 1535 pp (Cambridge University Press, Cambridge, United Kingdom and New York, NY, USA, 2013).

2 Hoffman, F. M. *et al.* Causes and implications of persistent atmospheric carbon dioxide biases in Earth System Models. *J. Geophys. Res.-Biogeo.* **119**, 141-162, doi:10.1002/2013JG002381 (2014).

3 Shevliakova, E. *et al.* Carbon cycling under 300 years of land use change: Importance of the secondary vegetation sink. *Global Biogeochem. Cy.* **23**, 1-16, doi:doi:10.1029/2007GB003176 (2009).

4 Andres, R. J. *et al.* A synthesis of carbon dioxide emissions from fossil-fuel combustion. *Biogeosciences* **9**, 1845-1871, doi:10.5194/bg-9-1845-2012 (2012).

5 Hurtt, G. *et al.* Harmonization of land-use scenarios for the period 1500–2100: 600 years of global gridded annual land-use transitions, wood harvest, and resulting secondary lands. *Climatic Change* **109**, 117-161, doi:10.1007/s10584-011-0153-2 (2011).

6 Moss, R. H. *et al.* The next generation of scenarios for climate change research and assessment. *Nature* **463**, 747-756, doi:http://www.nature.com/nature/journal/v463/n7282/suppinfo/nature08823_S1.html (2010).

7 Thomson, A. *et al.* RCP4.5: a pathway for stabilization of radiative forcing by 2100. *Climatic Change* **109**, 77-94, doi:10.1007/s10584-011-0151-4 (2011).

8 Di Vittorio, A. V. *et al.* From land use to land cover: restoring the afforestation signal in a coupled integrated assessment–earth system model and the implications for CMIP5 RCP simulations. *Biogeosciences* **11**, 6435-6450, doi:10.5194/bg-11-6435-2014 (2014).

9 Jones, A. D. *et al.* Greenhouse gas policy influences climate via direct effects of land-use change. *J. Climate* **26**, 3657-3670, doi:10.1175/JCLI-D-12-00377.1 (2013).

10 Ciais, P. *et al.* in *Climate Change 2013: The Physical Science Basis. Contribution of Working Group I to the Fifth Assessment Report of the Intergovernmental Panel on Climate Change* (eds T.F. Stocker *et al.*) (Cambridge University Press, Cambridge, United Kingdom and New York, NY, USA, 2013).

11 van Vuuren, D. *et al.* The representative concentration pathways: an overview. *Climatic Change* **109**, 5-31, doi:10.1007/s10584-011-0148-z (2011).

12 Meinshausen, M. *et al.* The RCP greenhouse gas concentrations and their extensions from 1765 to 2300. *Climatic Change* **109**, 213-241 (2011).

13 Lamarque, J.-F. *et al.* Global and regional evolution of short-lived radiatively-active gases and aerosols in the Representative Concentration Pathways. *Climatic Change* **109**, 191-212, doi:10.1007/s10584-011-0155-0 (2011).

14 Nelson, G. C. *et al.* Climate change effects on agriculture: economic responses to biophysical shocks. *Proc. Natl. Acad. Sci. U. S. A.* **111**, 3274-3279, doi:10.1073/pnas.1222465110 (2014).

15 Humpenöder, F. *et al.* Land-use and carbon cycle responses to moderate climate change: implications for land-based mitigation? *Environ. Sci. Technol.* **49**, 6731-6739, doi:10.1021/es506201r (2015).

16 Ruane, A. C. *et al.* Climate change impact uncertainties for maize in Panama: farm information, climate projections, and yield sensitivities. *Agr. Forest Meteorol.* **170**, 132-145, doi:http://dx.doi.org/10.1016/j.agrformet.2011.10.015 (2013).

17 Welch, J. R. *et al.* Rice yields in tropical/subtropical Asia exhibit large but opposing sensitivities to minimum and maximum temperatures. *Proc. Natl. Acad. Sci. U. S. A.* **107**, 14562-14567, doi:10.1073/pnas.1001222107 (2010).

18 Long, S. P., Ainsworth, E. A., Leakey, A. D. B., Nösberger, J. & Ort, D. R. Food for thought: lower-than-expected crop yield stimulation with rising CO_2 concentrations. *Science* **312**, 1918-1921, doi:doi: 10.1126/science.1114722 (2006).

19 Norby, R. J. *et al.* Forest response to elevated CO_2 is conserved across a broad range of productivity. *Proc. Natl. Acad. Sci. U. S. A.* **102**, 18052-18056 (2005).

20 Sutton, M. A. *et al.* Uncertainties in the relationship between atmospheric nitrogen deposition and forest carbon sequestration. *Glob. Change Biol.* **14**, 2057-2063, doi:10.1111/j.1365-2486.2008.01636.x (2008).

21 Norby, R. J., Warren, J. M., Iversen, C. M., Medlyn, B. E. & McMurtrie, R. E. CO2 enhancement of forest productivity constrained by limited nitrogen availability. *Proc. Natl. Acad. Sci. U. S. A.* **107**, 19368-19373, doi:10.1073/pnas.1006463107 (2010).

22 Rosenzweig, C. *et al.* Assessing agricultural risks of climate change in the 21st century in a global gridded crop model intercomparison. *Proc. Natl. Acad. Sci. U. S. A.* **111**, 3268-3273, doi:10.1073/pnas.1222463110 (2014).

23 Stehfest, E. *et al. Integrated Assessment of Global Environmental Change with IMAGE 3.0. Model description and policy applications.*, 370 pp (The Hague: PBL Netherlands Environmental Assessment Agency, 2014).

24 Voldoire, A., Eickhout, B., Schaeffer, M., Royer, J.-F. & Chauvin, F. Climate simulation of the twenty-first century with interactive land-use changes. *Clim. Dynam.* **29**, 177-193, doi:10.1007/s00382-007-0228-y (2007).

25 Wise, M., Calvin, K., Kyle, P., Luckow, P. & Edmonds, J. Economic and physical modeling of land use in GCAM 3.0 and an application to agricultural productivity, land, and terrestrial carbon. . *Clim. Change Econ.* **05**, 1450003, doi:10.1142/S2010007814500031 (2014).

26 Hurrell, J. W. *et al.* The Community Earth System Model: a framework for collaborative research. *B. Am. Meteorol. Soc.* **94**, 1339-1360, doi:10.1175/BAMS-D-12-00121.1 (2013).

27 Collins, W. D. *et al.* The integrated Earth System Model version 1: formulation and functionality. *Geosci. Model Dev.* **8**, 2203-2219, doi:10.5194/gmd-8-2203-2015 (2015).

28 Bond-Lamberty, B. *et al.* On linking an Earth system model to the equilibrium carbon representation of an economically optimizing land use model. *Geosci. Model Dev.* **7**, 2545-2555, doi:10.5194/gmd-7-2545-2014 (2014).

29 Stainforth, D. A., Allen, M. R., Tredger, E. R. & Smith, L. A. Confidence, uncertainty and decision-support relevance in climate predictions. *Philos. T. Roy. Soc. A* **365**, 2145-2161 (2007).

30 Strachan, N., Pye, S. & Kannan, R. The iterative contribution and relevance of modelling to UK energy policy. *Energ. Policy* **37**, 850-860, doi:http://dx.doi.org/10.1016/j.enpol.2008.09.096 (2009).

Acknowledgements

This work was supported by the U.S. Department of Energy, Office of Science, Office of Biological and Environmental Research, including support from the Accelerated Climate Modeling for Energy (ACME) project. This research used resources of the Oak Ridge Leadership Computing Facility, which is a U.S. Department of Energy Office of Science User Facility supported under Contract DE-AC05-00OR22725. This research used resources of the National Energy Research Scientific Computing Center, a DOE Office of Science User Facility supported by the Office of Science of the U.S. Department of Energy under Contract No. DE-AC02-05CH11231. This work used the Community Earth System Model, CESM and the Global Change Assessment Model, GCAM. The National Science Foundation and the Office of Science of the U.S. Department of Energy support the CESM project. The authors acknowledge long-term support for GCAM development from the Integrated Assessment Research Program in the Office of Science of the U.S. Department of Energy. Lawrence Berkeley National Laboratory is supported by the U.S. Department of Energy under Contract No. DE-AC02 0 5CH11231. Initial research by P.E.T., J.M., and X.S. was sponsored by the Laboratory Directed Research and Development Program of Oak Ridge National Laboratory, managed by UT-Battelle, LLC, for the U.S. Department of Energy. We thank Jay Gulledge for comments on the manuscript.

Author Contributions

W.D.C., J.E., A.T., B.B-L., A.D.J., and P.E.T. conceived the study. All authors contributed to development of algorithms. J.T. and A.C. led the software engineering development, X.S. configured and executed simulations, and M.L.B., J.M., K.C., L.C., B.B-L., and A.V.D.

performed diagnostics. All authors contributed to analysis of results. P.E.T., B.B.-L., A.D.J., A.V.D., K.C., L.C., X.S., and W.D.C. wrote the text, with comments and edits from all authors.

Competing Financial Interests

The authors declare no competing financial interests.

Figure Legends

Figure 1. Interactions between human and Earth systems using one-way (black) and two-way (black + red) coupling. a) Technological change factors for crop yield are included in the generation of IAMs used for AR5, but biospheric change factors are not. Demographic constraints and policy assumptions are necessary IAM inputs, with important influence on projected crop price, GHG emissions, and LULCC. Ecosystem productivity, including crop yield, has been considered as a static input to IAMs in AR5. Red arrows indicate the new feedback connections in our study, passing biospheric change information from the ESM back to the IAM through its influence on ecosystem productivity and crop yield. b) For AR5, connections across the dotted line are asynchronous and one-way (from IAM to ESM). Synchronous two-way coupling described here is accomplished by passing biospheric information, as filtered by the ESM land model component, to the IAM on a 5-year time step (red arrows, pathway labeled 1). This new information drives LULCC changes that are passed back to the land system (pathway labeled 2), resulting in a coupled feedback (green arrow). T, P, q, and rad indicate temperature, precipitation, humidity, and radiation components of physical climate.

Figure 2. Integrated biospheric change for the 21st century, as communicated from ESM to IAM. The scalar used to inform ecosystem productivity and crop yield changes in the IAM includes a vegetation component (shown here) based on change in net primary production relative to conditions in 1990 and a below ground component based on changes in net primary production and heterotrophic respiration (Supplemental Figure 1). Category “Other” includes urban, lake, land ice, and bare ground. The signal communicated to the IAM is specific to each agro-ecological zone and vegetation type within zone, with the plot showing an area-weighted global mean signal. For each aggregated land type the solid colored line shows the mean of two ensemble simulations, while the shaded region of matching color shows the range of values from the two ensemble members.

Figure 3. Changes in crop price and land-use area resulting from biospheric feedback. a) Percentage change in global average crop price, relative to the asynchronous one-way coupling (control) simulation, for each major crop type. b) Global total change in land cover summarized by major land-use/land-cover types, relative to the asynchronous one-way coupling simulation. For each aggregated crop type or land cover type the solid colored line shows the mean of two ensemble simulations, while the shaded region of matching color shows the range of values from the two ensemble members.

Figure 4. Change in global carbon stocks caused by biospheric feedback to human systems. Difference in total carbon stocks on land (Lnd), in the atmosphere (Atm), and in the oceans (Ocn), between two-way and one-way coupling simulations, as predicted within the ESM component of the coupled system. Solid colored line shows the mean of two ensemble members, while the shaded region of matching color shows range of values from the two ensemble members.

Online-Only Methods

Technical description of the two-way coupled system

A complete technical description for our two-way coupling framework (iESM) is published[27], including the model formulation, requirements, implementation, testing, and functionality.

Data availability

The complete iESM source code used to generate results for this study is available online at https://github.com/ACME-Climate. All model input data used in the simulations for this study, and all model output data used to generate the results reported here are available by request from the corresponding author.

Experimental design

Our simulation experiments are initiated with radiative forcing conditions estimated circa 1850 AD. The 1850 initial conditions for the ESM component (land, atmosphere, ocean, and sea ice state variables) are drawn from a long preindustrial control simulation (PC), in which the carbon cycle on land and in the atmosphere and oceans is fully prognostic. This PC simulation is over 1000 years long, with predicted atmospheric CO_2 concentration varying between 281 and 287 ppm. Experimental simulations used in this study were performed for two time segments: a historical transient (HT) segment covering the period 1850-2004, and a future scenario (FS) segment covering the period 2005 to 2094.

During HT segments only the ESM (in our case the Community Earth System Model, CESM) is active. Model inputs during HT segments, including fossil fuel emissions and land use and land cover change (LULCC)[5] are identical to those used for historical simulations in the Climate Model Intercomparison Project (CMIP5).

Both ESM and IAM components are active for FS segments. We performed two types of simulation in FS segments, differing only in the coupling method between ESM and IAM. One method used asynchronous 1-way coupling (A1), in which the IAM is run in stand-alone mode for the entire segment, followed by a stand-alone run of the ESM that receives LULCC and emissions information saved from the IAM simulation. This is the traditional coupling approach used for all CMIP5 future scenario simulations, and represented by the black arrows in Figure 1 (main text). The second method used synchronous 2-way coupling (S2) between the IAM and ESM, corresponding to the black and red arrows in Figure 1 (main text). The S2 coupling method is implemented exactly as described in the iESM technical description[27], except that our study used a 5-year coupling time step between IAM and ESM instead of the 15-year timestep described previously.

To ensure that the S2 coupling influence is restricted only to the passing of climate change information into the crop yield and carbon stock calculations of the IAM, we use identical anthropogenic fossil fuel and industrial emissions and other externally imposed radiative forcing agents as input to all FS segments. The inputs used were those generated by the GCAM model for the Reference Concentration Pathway (RCP) 4.5 as used in CMIP5[6]. To further constrain the two-way coupled experiment, we used the GCAM carbon price pathway generated in stand-alone mode (A1 type coupling) as a specified carbon price pathway for all FS segments. This allows us to interpret any differences between S2 and A1 coupling methods as arising from the direct influence of climate change on crop yields and carbon stocks in GCAM and the subsequent influence of those changes on land-use and land-cover change predictions, without needing to consider potential interactions with changing carbon price paths.

Our general approach to quantifying the influence of S2 vs. A1 coupling is to examine the difference between two FS simulation segments, one generated using the A1 approach (FS_A1) and another generated using the S2 approach (FS_S2). We refer to the difference between two such FS segments as our experimental result (ER = FS_S2 – FS_A1).

Each ER includes spatio-temporal variation generated by the difference in coupling methods and additional spatio-temporal variation generated by different realizations of the internal variability in the ESM. By generating multiple ensemble members of ER, we can evaluate the relative contributions of forced variation (the signal of interest in our analysis) and internal variation.

For this study we generated two ER ensemble members by initiating two separate HT segments from different time points, ten years apart, in the PC simulation (HTa and HTb). We then generated two FS segments starting from the endpoint of HTa, one using A1 coupling (FSa_A1) and the other using S2 coupling (FSa_S2). We generated a third FS segment from the endpoint of HTb, using S2 coupling (FSb_S2). The two ER ensemble members were then generated as ER1 = FSa_S2 – FSa_A1, and ER2 = FSb_S2 – FSa_A1.

Crop yields and bioenergy production in our coupled system are calculated in the IAM component. Crop yields in GCAM are calibrated against global crop data for years 1990 and 2005[31, 32]. As the S2 segments progress these yields are modified by climate change information passed back from the ESM. Evaluation of predicted yield by region and crop for years outside the calibration period shows reasonable model performance for present-day conditions [Supplemental Figure 8].

The influences of spatially and temporally evolving climate change factors on crop yields and bioenergy production are estimated within the ESM component of our coupled system and passed as scalars (multipliers) applied to yields in the IAM component. This coupling arrangement is outlined in Figure 1 (main text) and described in detail in the iESM technical documentation[27]. The ESM serves as an integrator of multiple climate change factors, but it is also of interest to isolate and assess contributions from individual factors. Given the uncertain magnitude of CO_2 fertilization effects on crop yields[18], it is of special interest to examine this factor in isolation and compare to experimental estimates as possible.

Our study concludes that synchronous two-way coupling generates significant changes in crop yields which propagate to influence crop prices, land use patterns, energy production, and fossil fuel emissions. Since these diagnosed changes are due to overall increases in crop yield and bioenergy production, it is possible that an overestimation of the CO_2 fertilization effect in crops by the ESM could lead to an overstatement of the significance of two-way coupling effects. As pointed out in the main text, our ESM component is one of a small number of such models that includes the limiting influence of mineral nutrient availability on land ecosystem processes. Coupling between the model representations of carbon and nutrient (nitrogen) cycles is directly responsible for a significant reduction in the CO_2 fertilization effect predicted at a given CO_2 concentration when compared to the same model with nutrient limitation switched off[33], and when compared to other models that lack nutrient limitation[10]. We can assert on this basis that of all the existing ESMs that might be evaluated in a two-way coupling context, CESM is among the two or three least likely to generate this type of overstatement of coupling effects due to high bias in CO_2 fertilization.

Even though CESM has a CO_2 fertilization effect 2.5 times smaller than the mean of the non-nutrient limited models[10], it is still possible that it overestimates the influence of CO_2 fertilization on crop yield compared to free-air concentration enrichment (FACE) experiments as summarized for example by Long et al.[18] To help further quantify this analysis, we refer to previously published results from a series of single factor experiments[28] which included the influence of historical changes in CO_2 concentration as one of the isolated factors. These results are based on simulations with CESM in which the land component is forced with a multi-year repeating cycle of surface weather data, while other factors such as CO_2 concentration, nitrogen deposition, or land use are allowed to vary (one at a time) according to their observed historical trajectories over the years 1850-2010.

In those simulations a gradual rise in CO_2 concentration of 110 ppmv (from 280 ppmv in year 1850 to 390 ppmv in year 2010) produced a ~7% increase in gross primary production (photosynthesis) and in net primary production (NPP, or vegetation growth). That simulation result is not directly comparable to the FACE experimental regime, since the model result is based on a gradual increase in CO_2 while the FACE experiments involve a step-change. Also, the FACE experiments started from modern CO_2 concentrations and increased concentration by about 200 ppmv, arriving at values around 550 ppmv. Chamber studies suggest that crop yield responses to CO_2 concentrations between 380 and 600 ppmv are approximately linear, and our offline model results are linear over the range 280 to 390 ppmv. It is reasonable to estimate, based on simple linear scaling, that the ~7% increase in NPP for the increase in atmospheric CO_2 from 280 to 390 ppmv would correspond to an increase in NPP of 12% for an increase in CO_2 similar to the FACE experiments. We are not able to quantify the potential influence of gradual vs. step change in CO_2 concentration from the available results.

Since NPP from CESM is passed to the IAM in our synchronously coupled system as a scalar (multiplier) on crop yields, a useful comparison with FACE results is from a synthesis for CO_2 enrichment effects on crop yields[18], which summarized the FACE results for rice, wheat and soybean yields as 12%, 13%, and 14% increase, respectively. The major difference between our model results and the FACE crop synthesis[18] is for C_4 crops. CESM includes a C_4 grass type, and although the underlying physiology model does not predict a significant response to CO_2 fertilization in this type through an influence on leaf-scale photosynthetic rate, effects of CO_2 concentration on stomatal conductance are included for C_4 types, and NPP increases for C_4 types in the single-factor experiment are similar to increases for C_3 types due to indirect effects on soil water status. This is in contrast to the FACE synthesis, which found no effect of enriched CO_2 concentration on C_4 crop yield (based on one year of data from one study).

In follow-on work, we are improving the representation of multiple crop types directly within the ESM component, so that information can be passed with less aggregation between the ESM and IAM components in future coupling simulations.

We include a single pair of simulation experiments for the RCP 8.5 scenario, as a preliminary test of the generality of our RCP 4.5 results. The RCP 8.5 simulations start from the same HT endpoint as described above for RCP 4.5, and follow a common simulation protocol. Only one A1 and one S2 simulation was performed for RCP 8.5, so the results described in the main text and illustrated in Supplemental Figure 8 reflect only a single ensemble member.

Additional References for Online-Only Methods

31 FAOSTAT. Food and Agriculture Organization of the United Nations. Rome, Italy. (faostat3.fao.org) (2014)

32 Kyle, P. *et al. GCAM 3.0 Agriculture and Land Use: Data Sources and Methods.* Richland, WA, Pacific Northwest National Laboratory. (2011)

33 Thornton, P. E., J.-F. Lamarque, N. A. Rosenbloom and N. M. Mahowald. Influence of carbon-nitrogen cycle coupling on land model response to CO2 fertilization and climate variability. *Glob. Biogeochem. Cy.* **21**(4): GB4018 doi:10.1029/2006GB002868. (2007)

Figure 1a

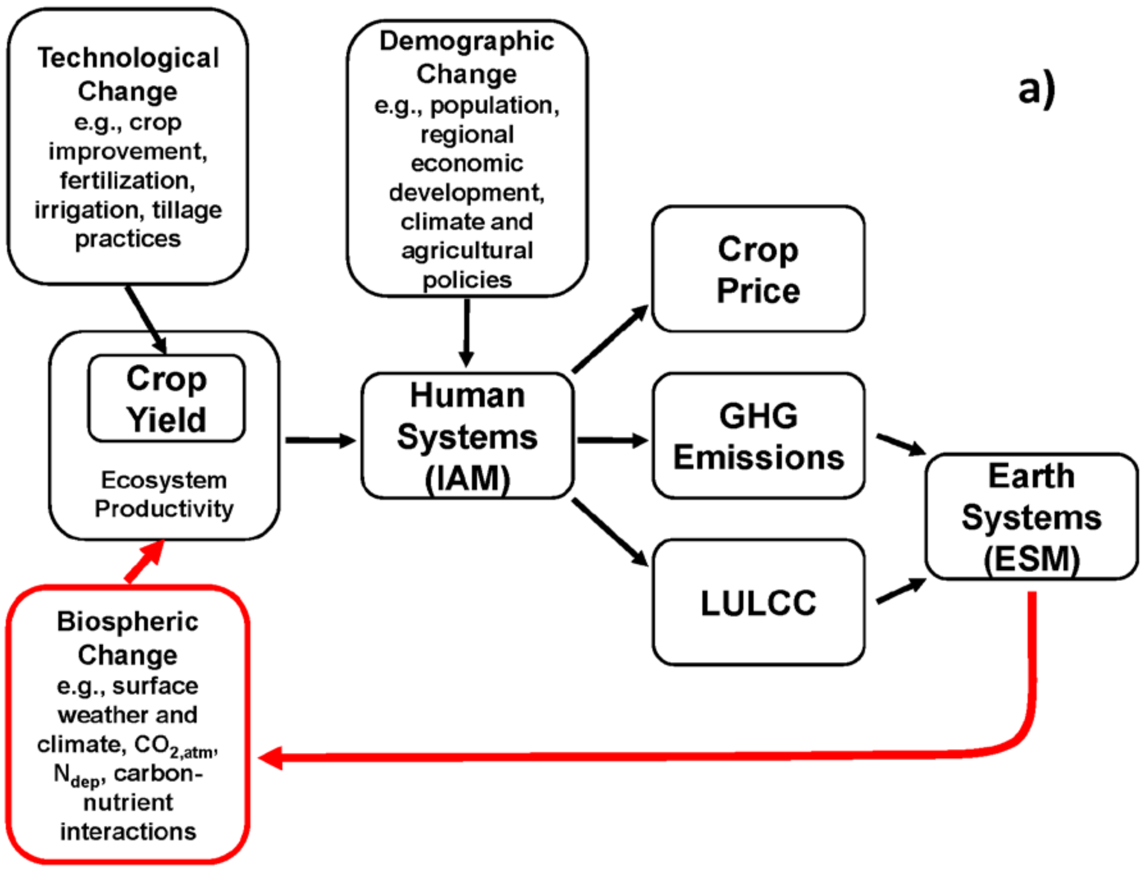

a)
Technological Change
e.g., crop improvement, fertilization, irrigation, tillage practices
Demographic Change
e.g., population, regional economic development, climate and agricultural policies
Crop Yield
Ecosystem Productivity
Human Systems (IAM)
Crop Price
GHG Emissions
LULCC
Earth Systems (ESM)
Biospheric Change
e.g., surface weather and climate, $CO_{2,atm}$, N_{dep}, carbon-nutrient interactions

Figure 1b

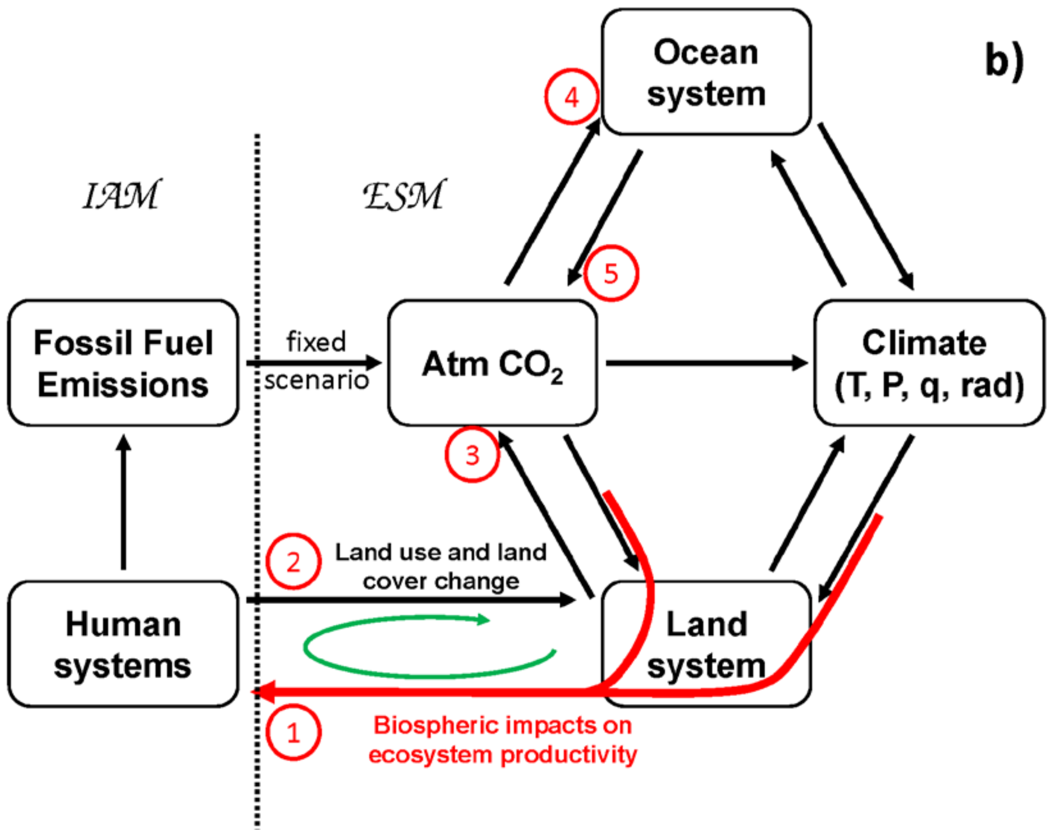
b)
IAM
ESM
Ocean system
Fossil Fuel Emissions
fixed scenario
Atm CO_2
Climate (T, P, q, rad)
Human systems
Land use and land cover change
Land system
Biospheric impacts on ecosystem productivity
1
2
3
4
5

Figure 2

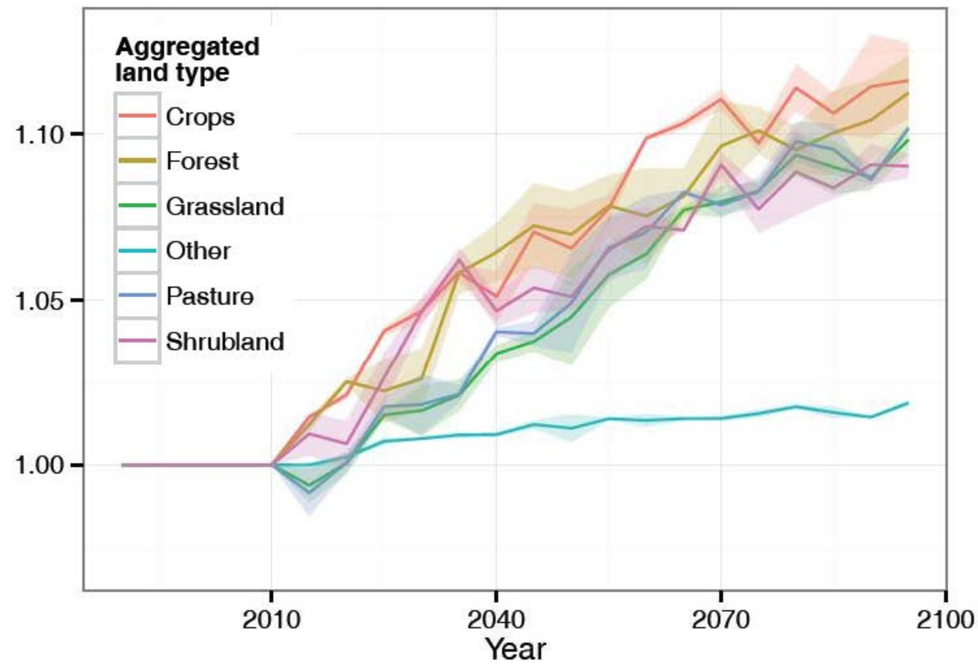
Aggregated
land type
Crops
Forest
Grassland
Other
Pasture
Shrubland
1.10
1.05
1.00
2010
2040
2070
2100
Year

469 Figure 3a

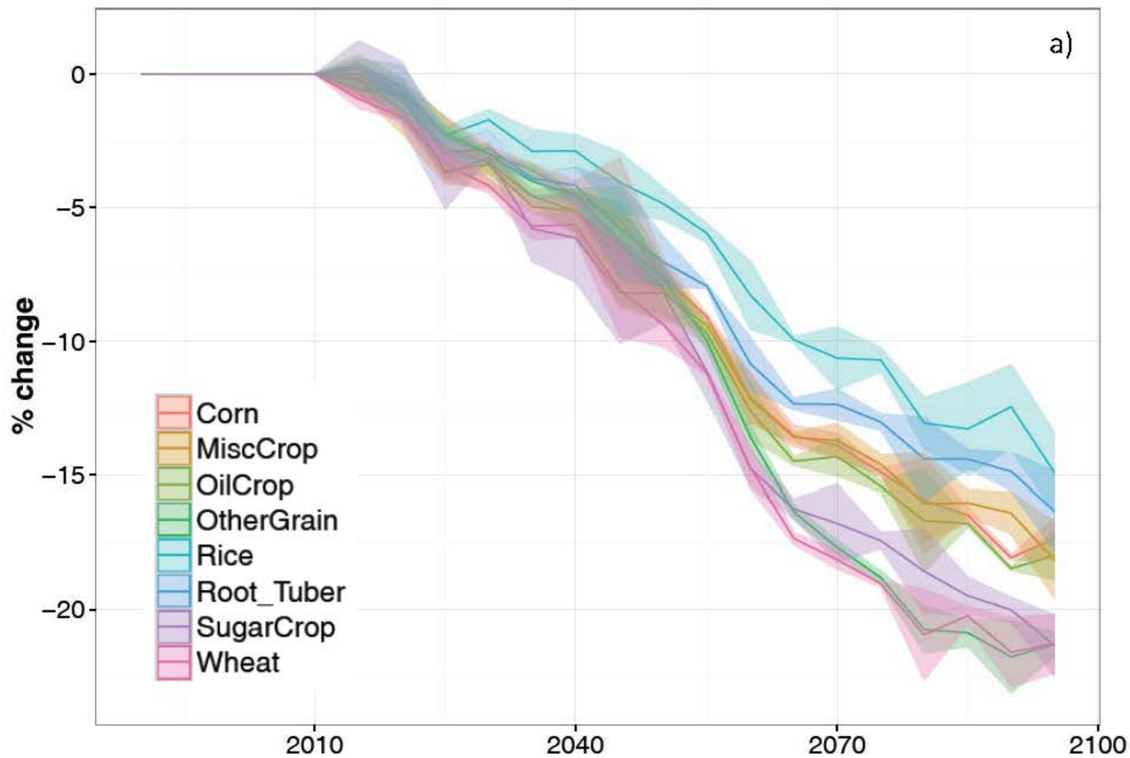

470

471

Figure 3b

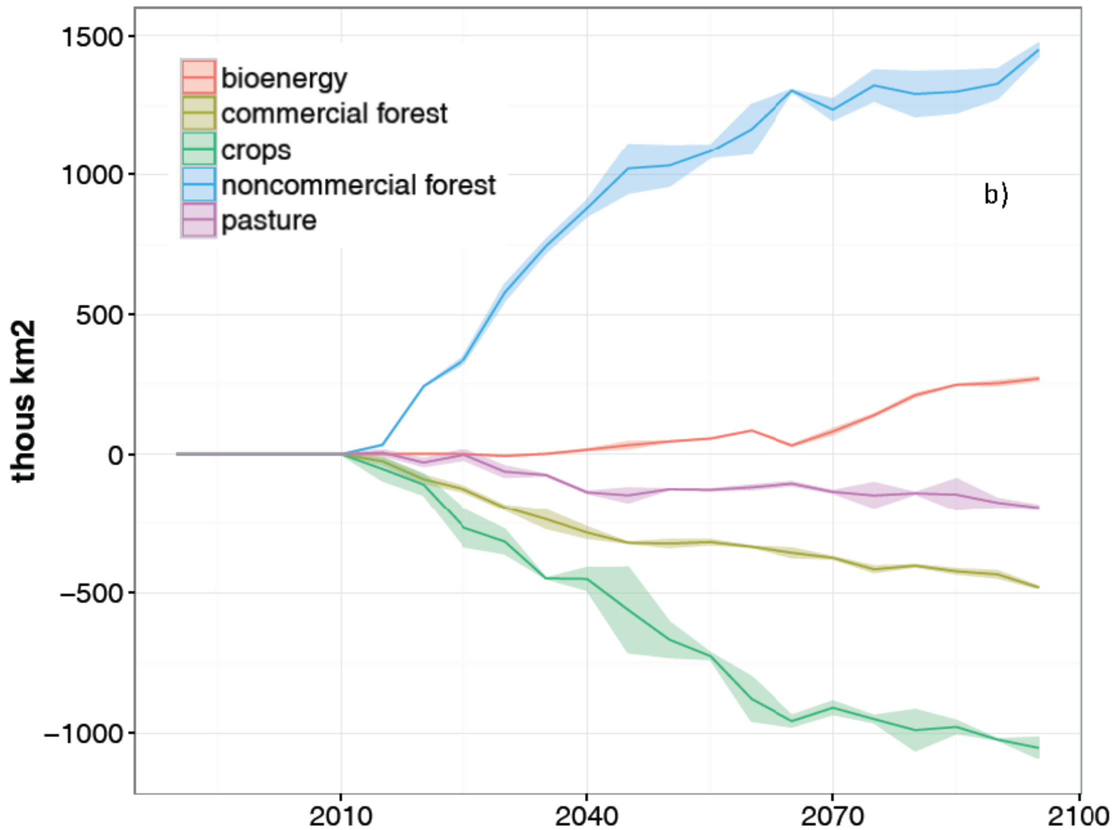
bioenergy
commercial forest
crops
noncommercial forest
pasture
b)
thous km2
1500
1000
500
0
−500
−1000
2010
2040
2070
2100

Figure 4

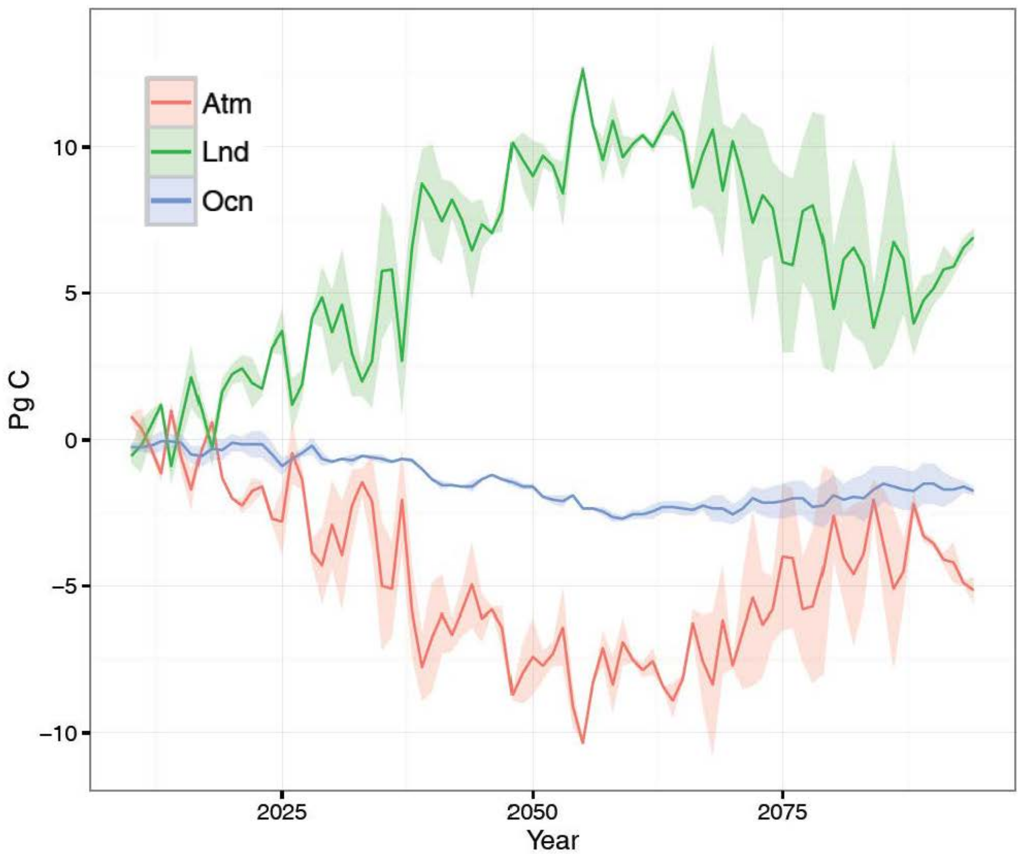

Biospheric feedback effects in a synchronously coupled model of Earth and human systems

Supplementary Information

Supplementary Information for this study consists of eight figures and their captions.

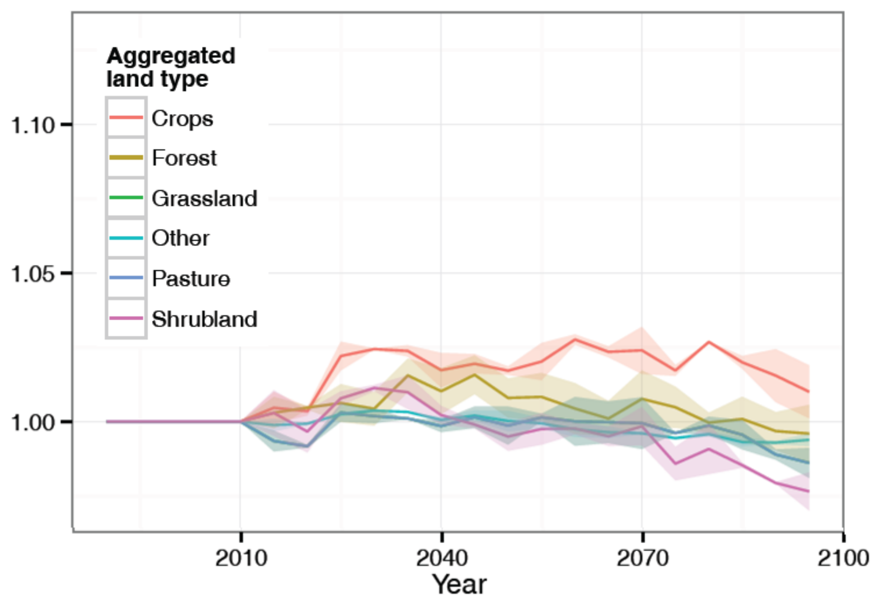

Supplemental Figure 1. Soil component of the integrated biospheric change signal passed from ESM to IAM, based on changes in belowground net primary production and heterotrophic respiration in the ESM relative to conditions in 1990. Signal communicated to IAM is specific to each agro-ecological zone and vegetation type within zone, with the plot showing an area-weighted global mean signal. For each aggregated land type the solid colored line shows the mean of two ensemble simulations, while the shaded region of matching color shows the range of values from the two ensemble members.

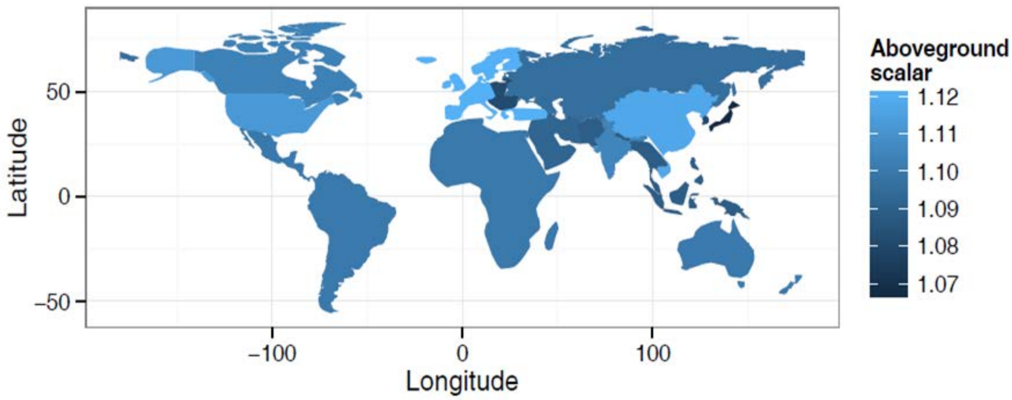

Supplemental Figure 2. Regional means for the aboveground component of integrated biospheric change signal in simulation year 2094.

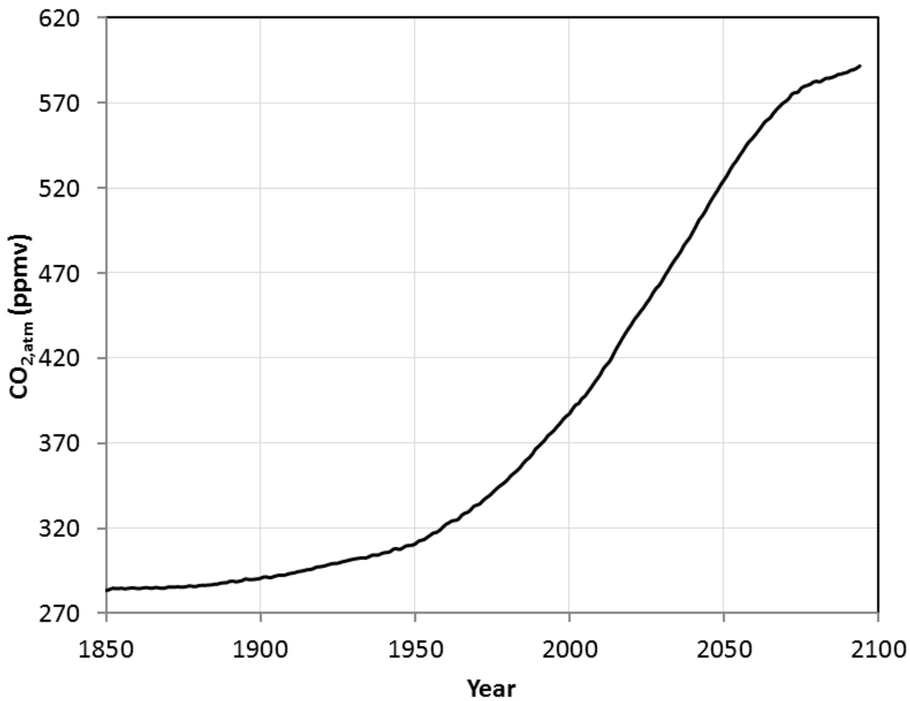

Supplemental Figure 3. Global mean near-surface atmospheric CO_2 from the historical transient simulation (1850-2004) and a two-way synchronous coupling experiment (2005-2094).

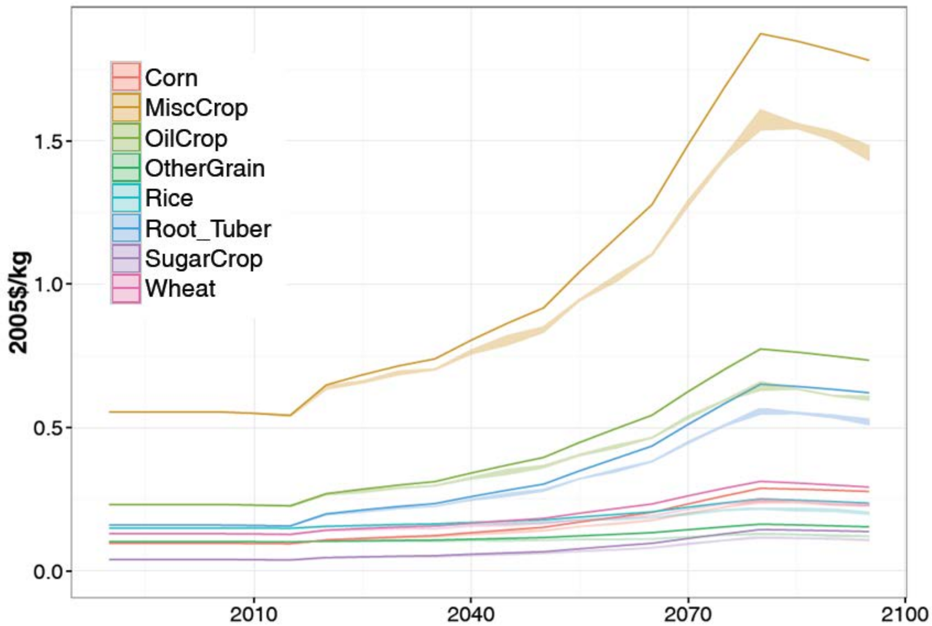

Supplemental Figure 4. Crop prices (in 2005$/kg) for two-way coupled (shaded regions) and one-way coupled (solid lines) simulations for several major crop types. For each crop type the shaded region shows the range of values from the two ensemble members.

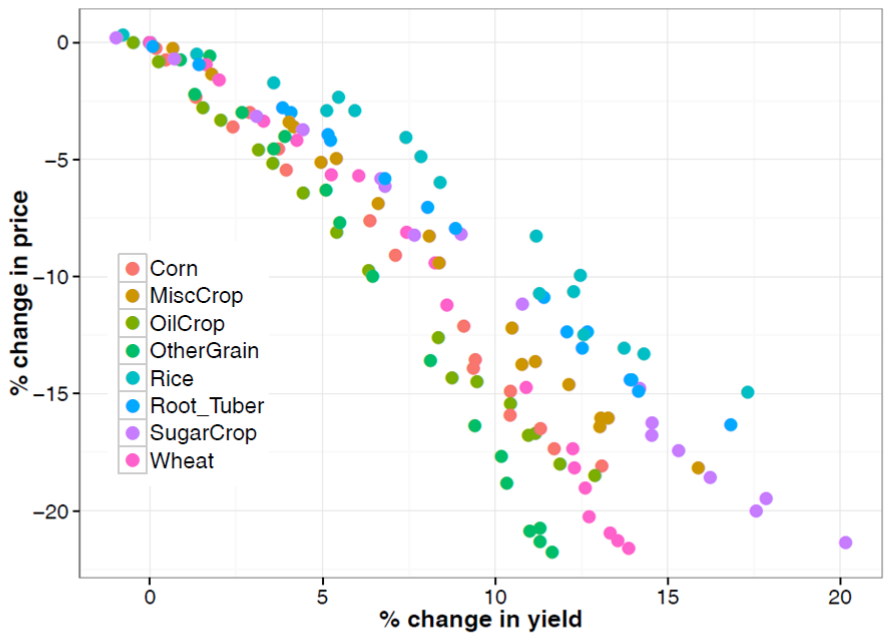

Supplemental Figure 5. Change in price for major crop types shown as a function of change in yield for each crop type. Each point represents a single five-year time period (2005-2094) from one ensemble simulation for a single crop, with changes shown as percent difference between two-way synchronous coupled and one-way asynchronous coupled simulations. The plot includes points from both ensemble simulations.

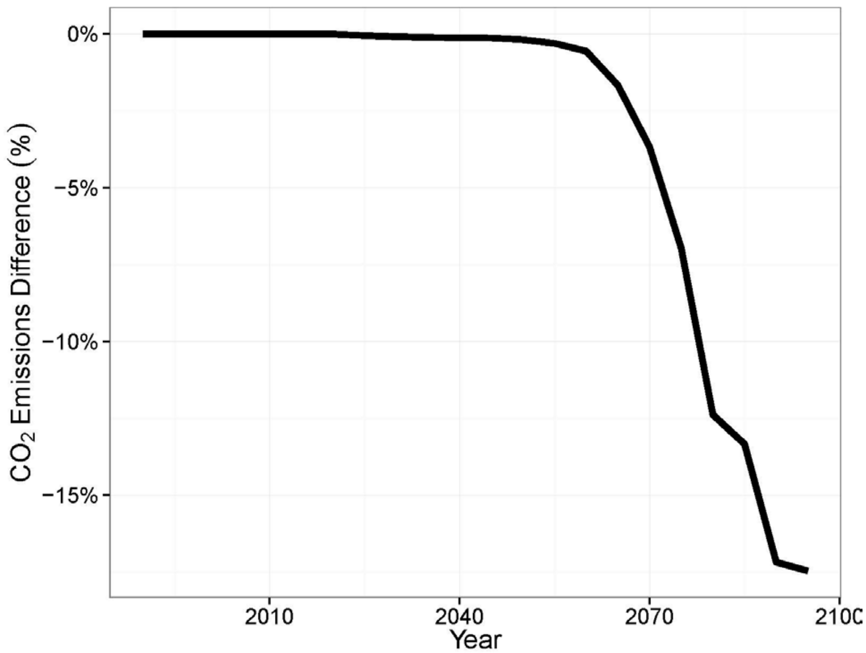

Supplemental Figure 6. Difference in fossil fuel CO_2 emissions as a result of biospheric change feedback, shown as a percentage change between the two-way synchronous coupling and one-way asynchronous coupling simulations.

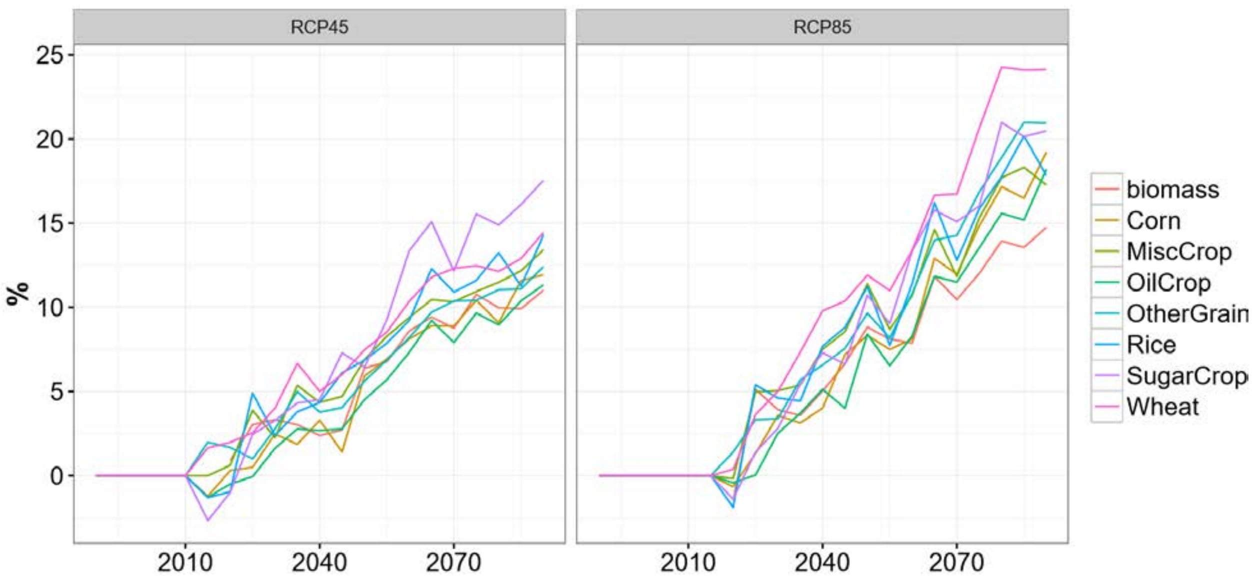

Supplemental Figure 7. Percent change in global mean yield for multiple crop types in the synchronous two-way coupling experiment compared to the asynchronous one-way coupling experiment, showing results for RCP 4.5 (left) and RCP 8.5 (right). Although RCP 8.5 has significantly higher $CO_{2,atm}$ at the end of century than RCP 4.5, crop yields are only modestly higher due to the offsetting influence of more extreme radiatively-forced climate changes under RCP 8.5.

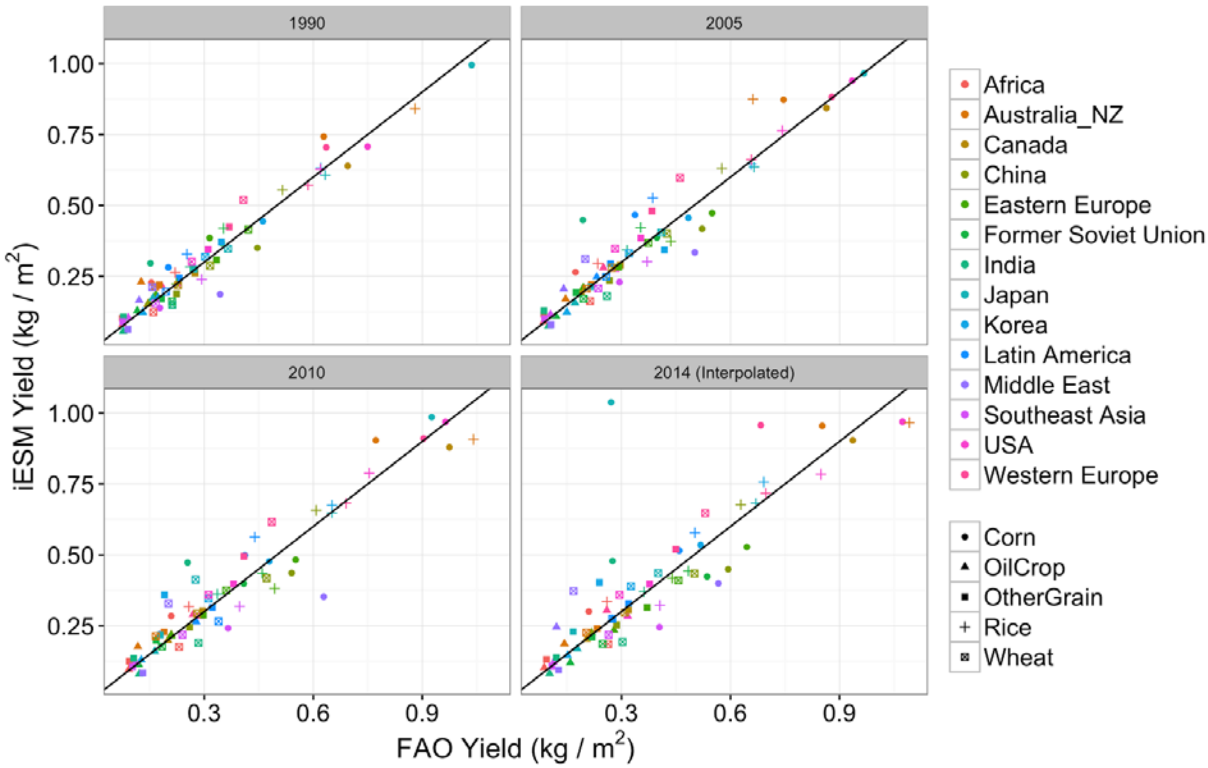

Supplemental Figure 8. Model-predicted vs. observed yield for five crops over multiple regions, for two calibration years (1990 and 2005), and two additional years (2010 and 2014). Model results for 2014 are interpolated from the actual model outputs in 2010 and 2015, to allow comparison with the most recent year for which FAO crop yield observations are available.